

AD-A285 930

REPORT DOCUMENTATION PAGE *Dist: A*Form Approved  
OMB No. 0704-0188

Public reporting burden for this collection of information is estimated to average 1 hour per response, including the time for reviewing instructions, searching existing data sources, gathering and maintaining the data needed, and completing and reviewing the collection of information. Send comments regarding this burden estimate or any other aspect of this collection of information, including suggestions for reducing this burden, to Washington Headquarters Services, Directorate for Information Operations and Reports, 1215 Jefferson Davis Highway, Suite 1204, Arlington, VA 22202-4302, and to the Office of Management and Budget, Paperwork Reduction Project (0704-0188), Washington, DC 20503.

1. AGENCY USE ONLY (Leave blank)		2. REPORT DATE		3. REPORT TYPE AND DATES COVERED ANNUAL	
4. TITLE AND SUBTITLE CORROSION OF AIRCRAFT MATERIALS: CORRELATION BETWEEN NANOMETER SCALE & MACROSCOPIC STRUCTURAL DAMAGE PARAMETERS				5. FUNDING NUMBERS F49620-94-C-0040 65502F 3005/SS	
6. AUTHOR(S) Dr A. Gonzales-Martin, D. Hodko, C. Andrews and O.J. Murphy					
7. PERFORMING ORGANIZATION NAME(S) AND ADDRESS(ES) Lynntech, Inc. 7610 Eastmark Drive, Suite 105 College Station, TX 77840				8. PERFORMING ORGANIZATION REPORT NUMBER AFOSR-TR- 94 0674	
9. SPONSORING/MONITORING AGENCY NAME(S) AND ADDRESS(ES) AFOSR/NL 110 Duncan Ave Suite B115 Bolling AFB DC 20332-0001 Maj Erstfeld				10. SPONSORING/MONITORING AGENCY REPORT NUMBER	
11. SUPPLEMENTARY NOTES					
12a. DISTRIBUTION AVAILABILITY STATEMENT This document has been approved for public release and sale; its distribution is unlimited.					
13. ABSTRACT (Maximum 200 words)  The following work has been carried out during the reporting period: (i) imaging of pitting corrosion initiation in aluminum at the nanometer scale, (ii) study of the effects of main atmospheric pollutants on the initiation of the corrosion process; (iii) identification of surface regions at an aluminum sample where corrosion is most likely to occur; (iv) measurements of the electrochemical impedance spectra on Al sample before and during the pitting process in NaCl; (v) identification of the impedance parameters characteristic for the pitting the corrosion of the aluminum sample.				12b. DISTRIBUTION CODE  A	
14. SUBJECT TERMS				15. NUMBER OF PAGES	
				16. PRICE CODE	
17. SECURITY CLASSIFICATION OF REPORT (U)	18. SECURITY CLASSIFICATION OF THIS PAGE (U)	19. SECURITY CLASSIFICATION OF ABSTRACT (U)	20. LIMITATION OF ABSTRACT (U)		

3

**CORROSION OF AIRCRAFT MATERIALS: CORRELATION  
BETWEEN NANOMETER SCALE AND MACROSCOPIC  
STRUCTURAL DAMAGE PARAMETERS**

Contract No.: F49620-94-C-0040

**FIRST BI-MONTHLY REPORT**

*Prepared by:*

A. Gonzalez-Martin, D. Hodko, C. Andrews, and O.J. Murphy

**Lynntech, Inc.**  
7610 Eastmark Drive, Suite 105  
College Station, TX 77840

**94-33889**



898

*Submitted to:*

MAG T. E. Eastfield

**U.S. Department of the Air Force**  
**AFOSR/NL**  
Air Force Office of Scientific Research  
110 Duncan Av., Suite B115  
Bolling AFB DC 20332-0001

August 15, 1994

Accession For	
NTIS CRA&I	<input checked="" type="checkbox"/>
DTIC TAB	<input type="checkbox"/>
Unannounced	<input type="checkbox"/>
Justification	
By	
Distribution/	
A-1	

94 11 1 06 3

28 SEP 1994

The following work has been carried out during the reporting period: (i) imaging of pitting corrosion initiation in aluminum at the **nanometer scale**; (ii) study of the effects of main atmospheric pollutants on the initiation of the corrosion process; (iii) identification of surface regions at an aluminum sample where corrosion is most likely to occur; (iv) measurements of the electrochemical impedance spectra on Al sample before and during the pitting process in NaCl; (v) identification of the impedance parameters characteristic for the pitting the corrosion of the aluminum sample.

**(i) Imaging of pitting corrosion initiation in aluminum at the nanometer scale by atomic force microscope (AFM).**

In this study, AFM NanoScope<sup>®</sup> III (Digital Instruments, CA) was used. AFM measures the attractive or repulsive force between a sharp tip (located at the end of a long cantilever with a low spring constant) and the sample which is used to image the surface topography. As with other scanning probe microscopes (SPMs), AFM allows three-dimensional imaging of surface structures atomic to micro scale. As opposed to optical and electron microscopes (e.g., scanning electron microscope, SEM, and transmission electron microscopes, TEM) which can be operated only in vacuum, SPMs can be used as well in air and in liquids.

As a standard procedure, the AFM NanoScope<sup>®</sup> III instrument was calibrated by the imaging of a graphite single crystal surface. Figure 1 shows the AFM image of that surface. Atomic resolution was obtained, and the lattice distance corresponded to the values reported in the literature (1).

Next, the imaging of a polished aluminum surface was carried out. The sample was prepared as follows. An aluminum disc, 6 mm diameter (AESAR, 99.9965%) was polished with 1  $\mu\text{m}$  diamond paste (Buehler) and then with silica gel (0.05  $\mu\text{m}$ , Buehler) until a mirror finished surface was obtained. Before the AFM imaging, the surface was cleaned with methanol. Figures 2 and 3 show the AFM imaging of the aluminum surface at two different resolutions at **nanometer scale**. At these high resolutions, some surface structures could be observed (e.g., small pits). This indicated that the previous surface treatment did not completely produce a flat surface<sup>1</sup>. Figure 3b shows a cross section of a deep pit from Figure 3a (cf., red arrows). The depth of the pit was about 5 nm, and the width was about 276.5 nm. The width to depth ratio of this pit was about 55.

**(ii) Study of the effects of main atmospheric pollutants on the corrosion process.**

To study the effect of some atmospheric pollutants on the corrosion process, an aluminum sample was exposed to 0.6 M NaCl solution. Figure 4 shows the cyclic voltammogram of the aluminum sample in the NaCl solution. The pitting potential was located at about -0.73 V/SCE. No active/passive transition region could be observed in

---

<sup>1</sup> These pits could be produced with the silica gel treatment.

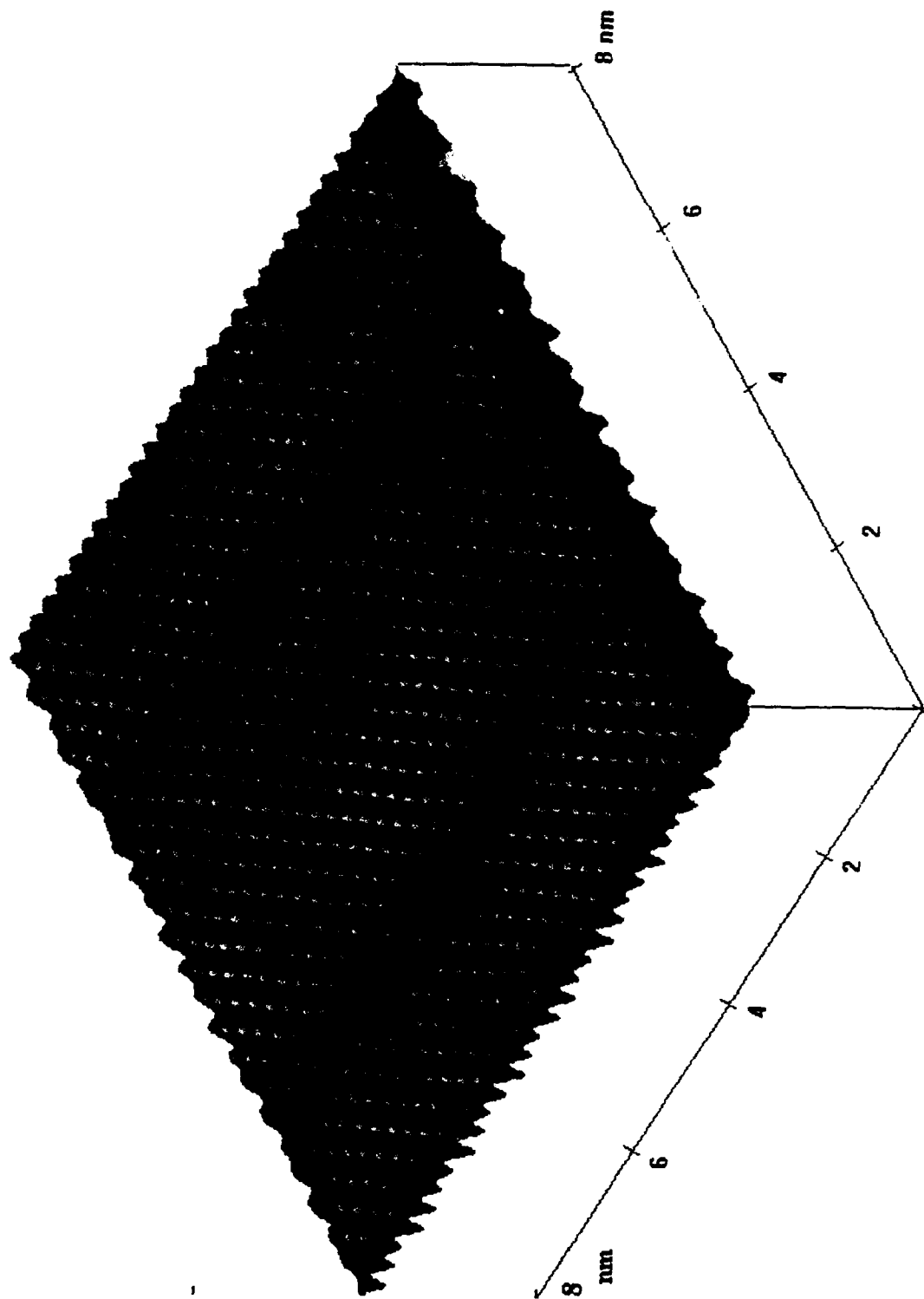


Figure 1. Atomic resolution image of a graphite single crystal surface obtained by AFM NanoScope III.

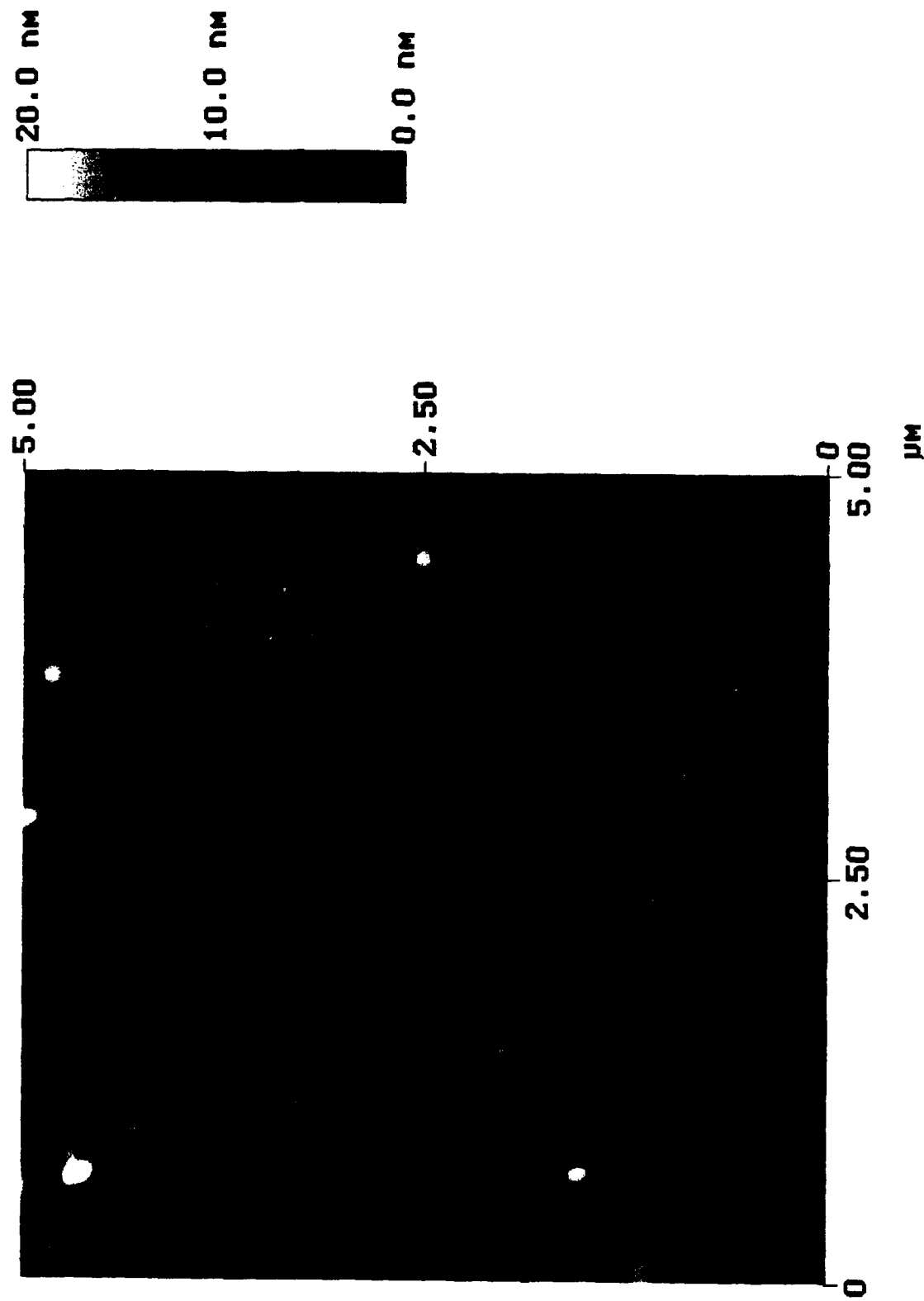


Figure 2. AFM image of an Al sample after the mirror finish polishing. Vertical scale is 20.0 nm.

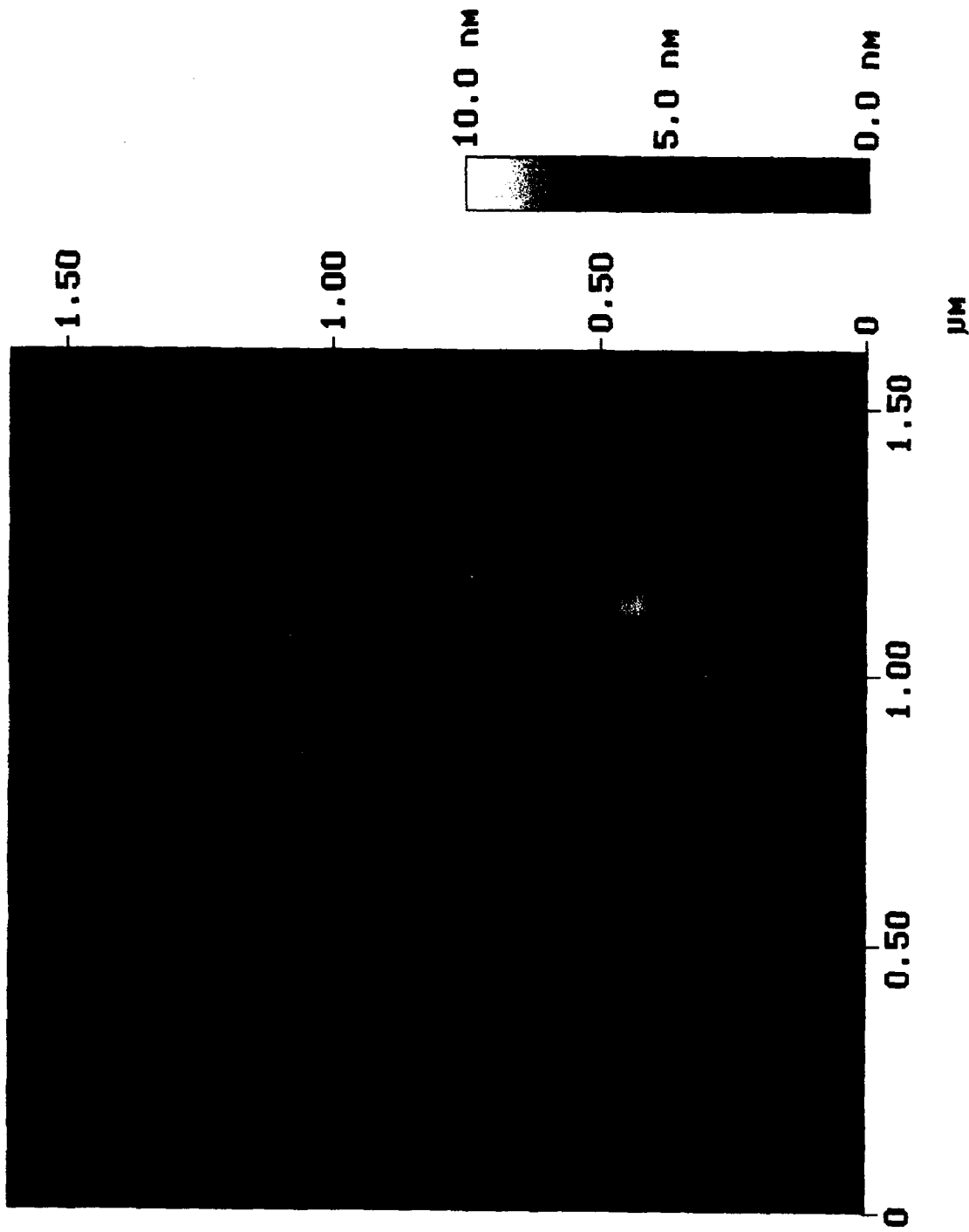


Figure 3a. AFM image of an Al sample after the mirror finish polishing. Vertical scale is 10.0 nm.

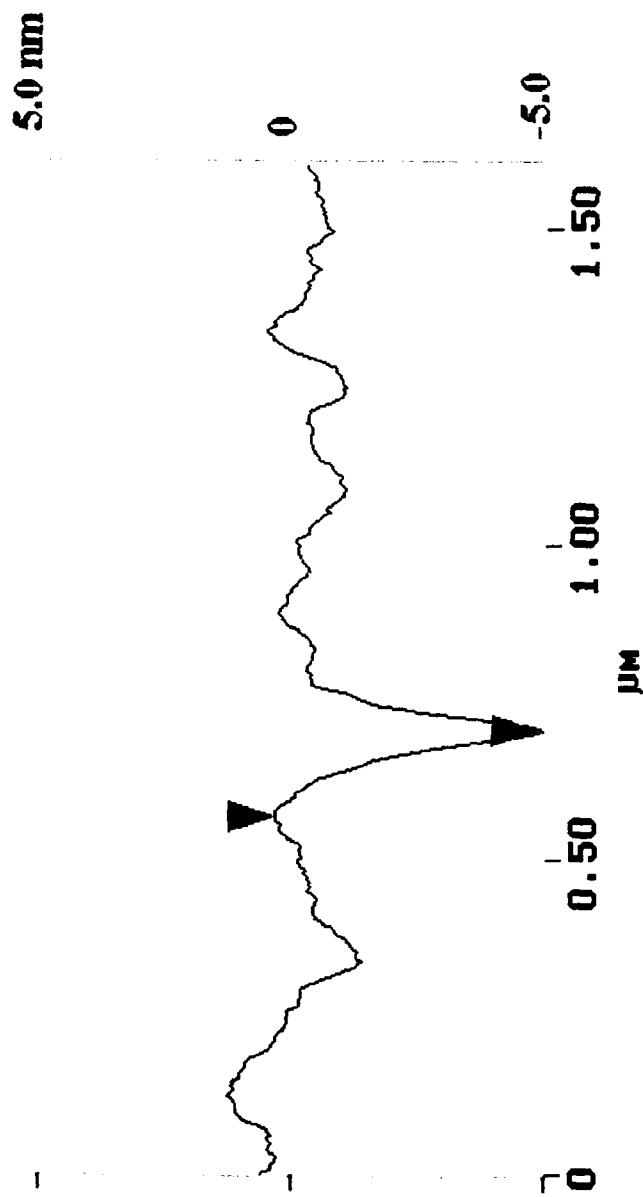


Figure 3b. Cross section of a deep pit from Figure 3a

(cf., red arrows).

the presence of the chloride ions. The electrochemical potential control at the electrode pitting potential allowed us to accelerate and manipulate the degree of corrosion of the aluminum sample.

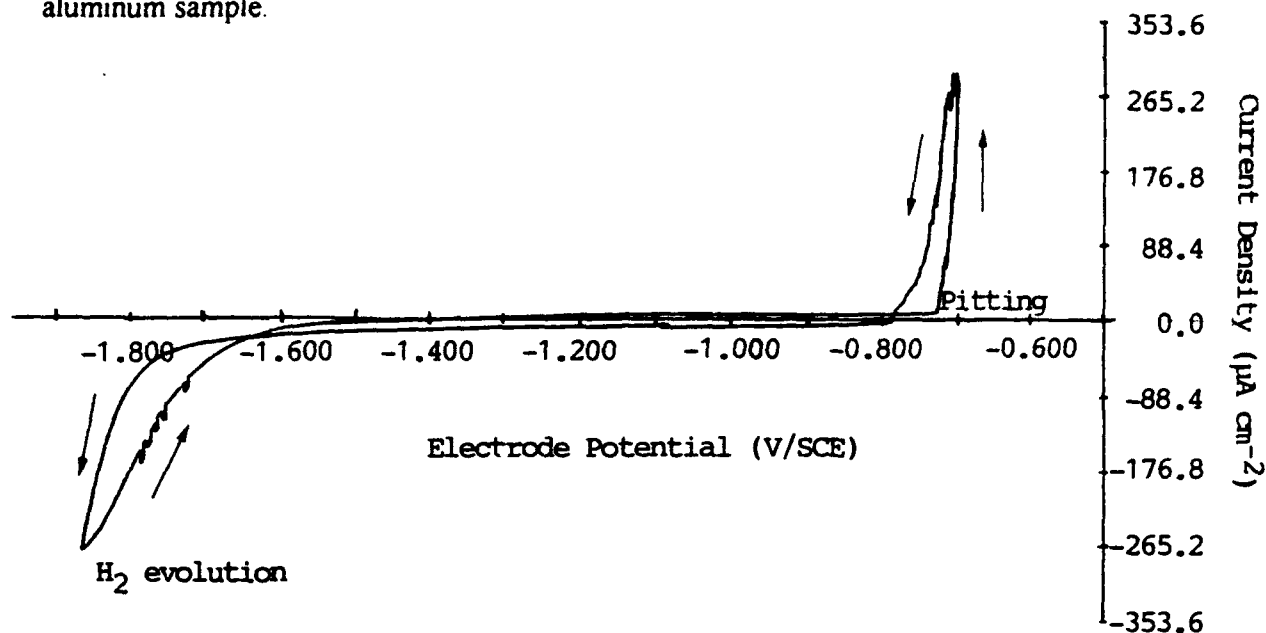


Figure 4. Cyclic voltammetry of aluminum in 0.6 M NaCl solution. Scan rate =  $5 \text{ mV s}^{-1}$ .

In order to obtain images of the corroded aluminum surface at the nanometer scale, a sample with a mirror surface finish was exposed to the NaCl solution and the corrosion process was accelerated by applying an electrochemical potential corresponding to the pitting potential (cf., Figure 4) for 1 minute. The surface of the sample was then inspected by AFM. Figures 5-7 show the AFM images of the corroded aluminum surface at different resolutions. Those figures can be compared with the AFM images of the non-corroded, polished aluminum surface (cf., Figures 2 and 3). Figure 5 is at the same horizontal resolution as Figure 2, although the vertical scale in Figure 5 is 2.5 times less sensitive. The AFM image of the electrochemically corroded surface shown in Figure 5 shows a surface with much more developed surface structures (e.g., pits) compared to a non-corroded surface shown in Figure 2, even at the lower vertical scale resolution. The same observation was obtained from Figure 6a. Compared with Figure 3a, Figure 6a shows a corroded surface with much higher density of pits and are also deeper pits. Figure 6b shows the cross section of several of those pits (cf., arrows). For some of those pits, the depth could not be determined for it was deeper than the instrument detection limit. For other pits, the width to depth ratio was about 17, smaller than that obtained before corrosion (c.f., Figure 3). Figure 7a shows two of the pits from Figure 6a at a higher magnification, and Figure 7b shows their cross section. The width to depth ratio was about 14. This ratio provides useful information on the mechanism of corrosion of the Al sample in the NaCl solution: the corrosion process is localized, and the growth of the pits



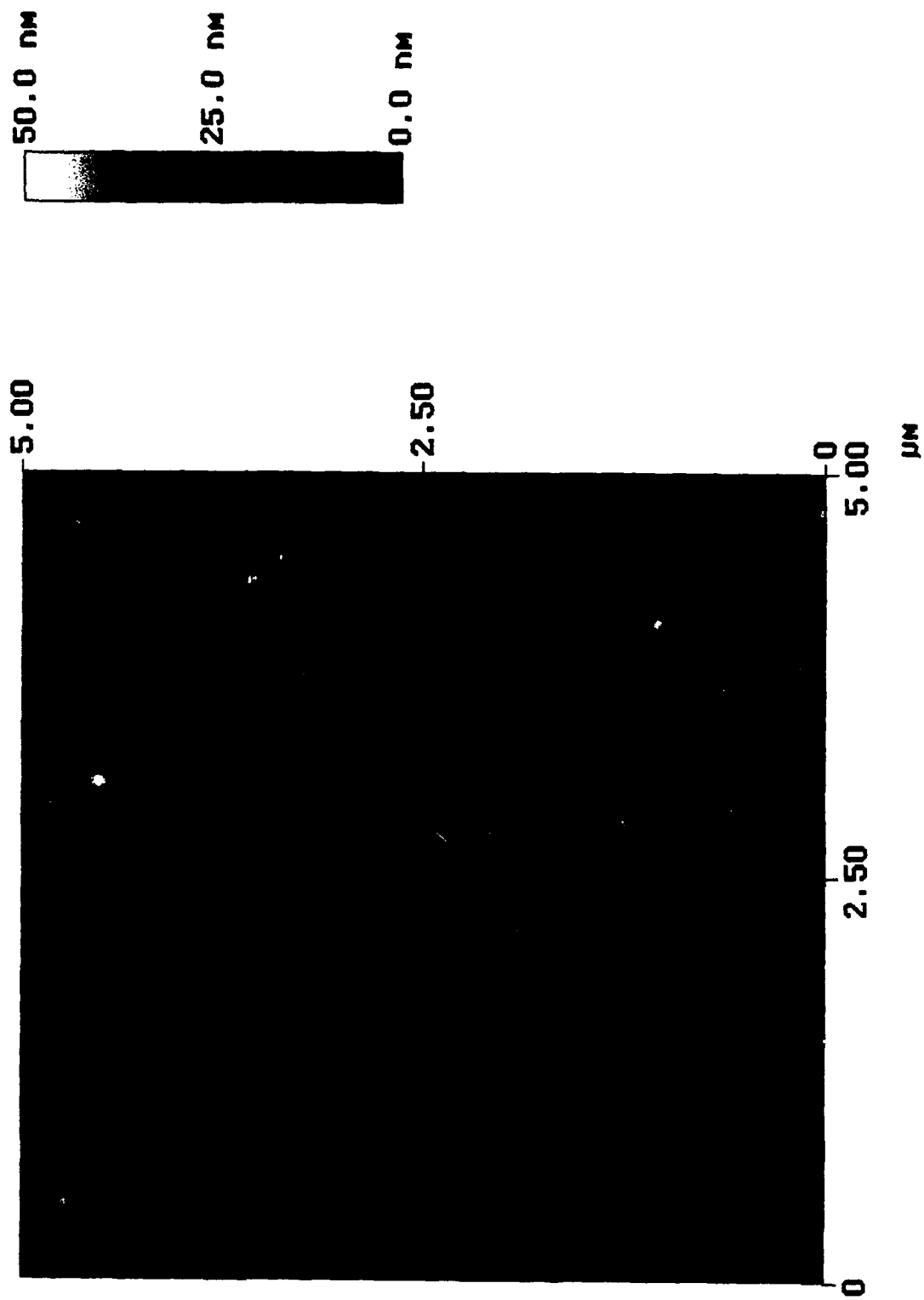


Figure 5. AFM image of an Al sample after electrochemically induced corrosion. Vertical scale is 50.0 nm.

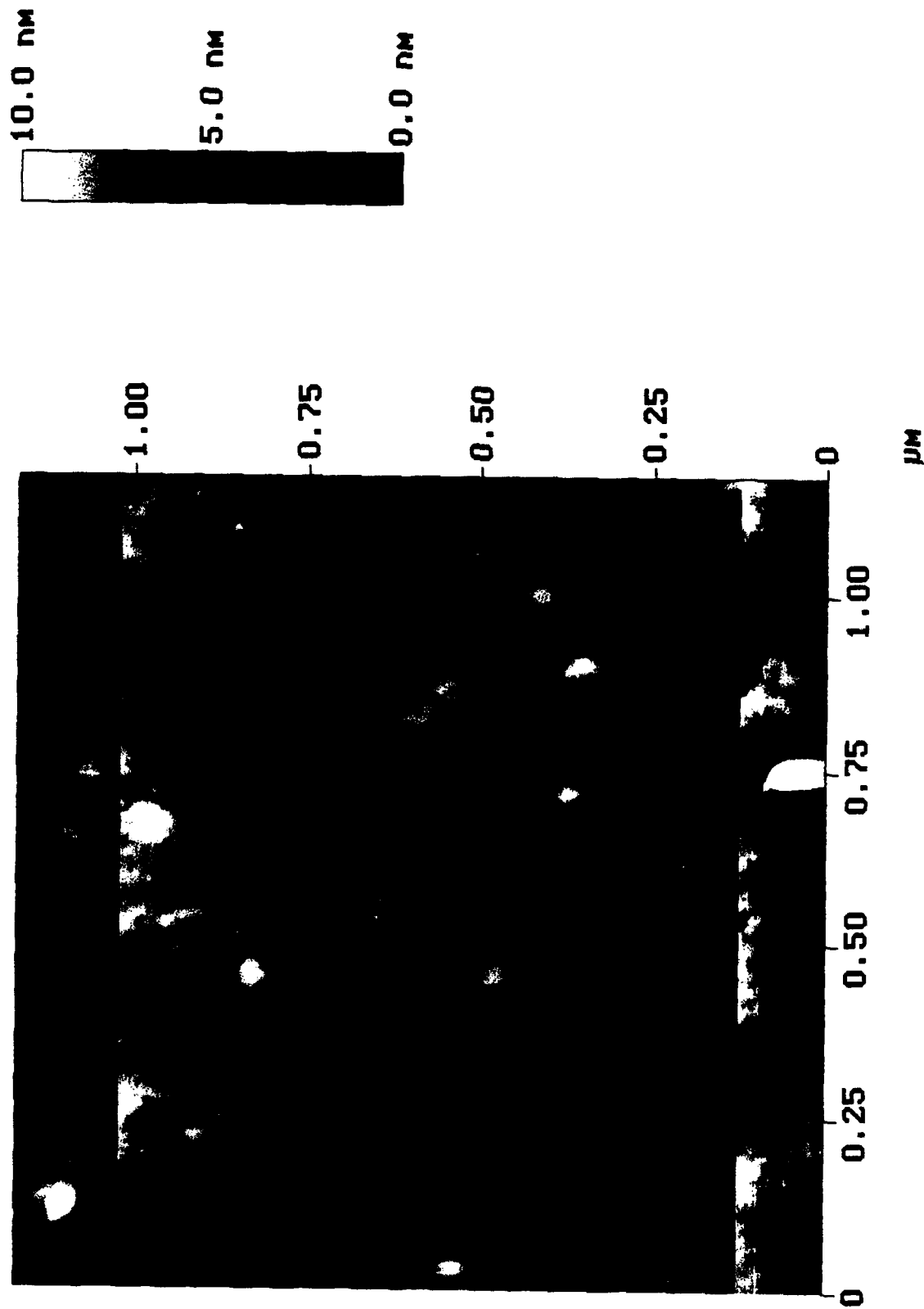


Figure 6a. AFM image (higher magnification) of an Al sample after electrochemically induced corrosion. Vertical scale is 10.0 nm.

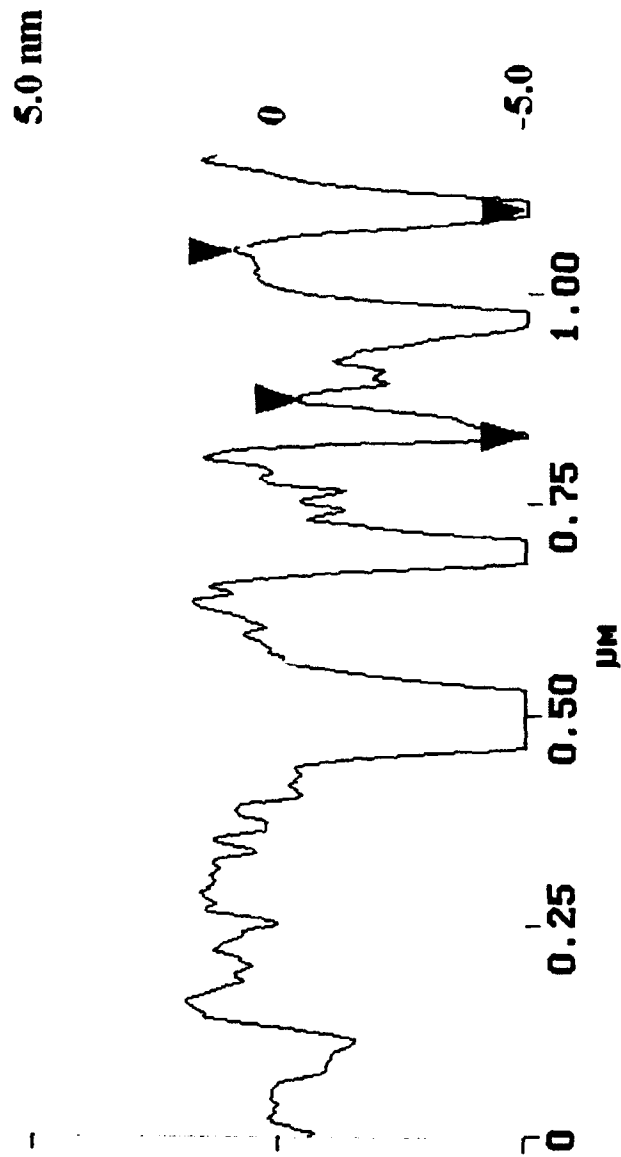


Figure 6b. Cross section of pits from Figure 6a (through red line).

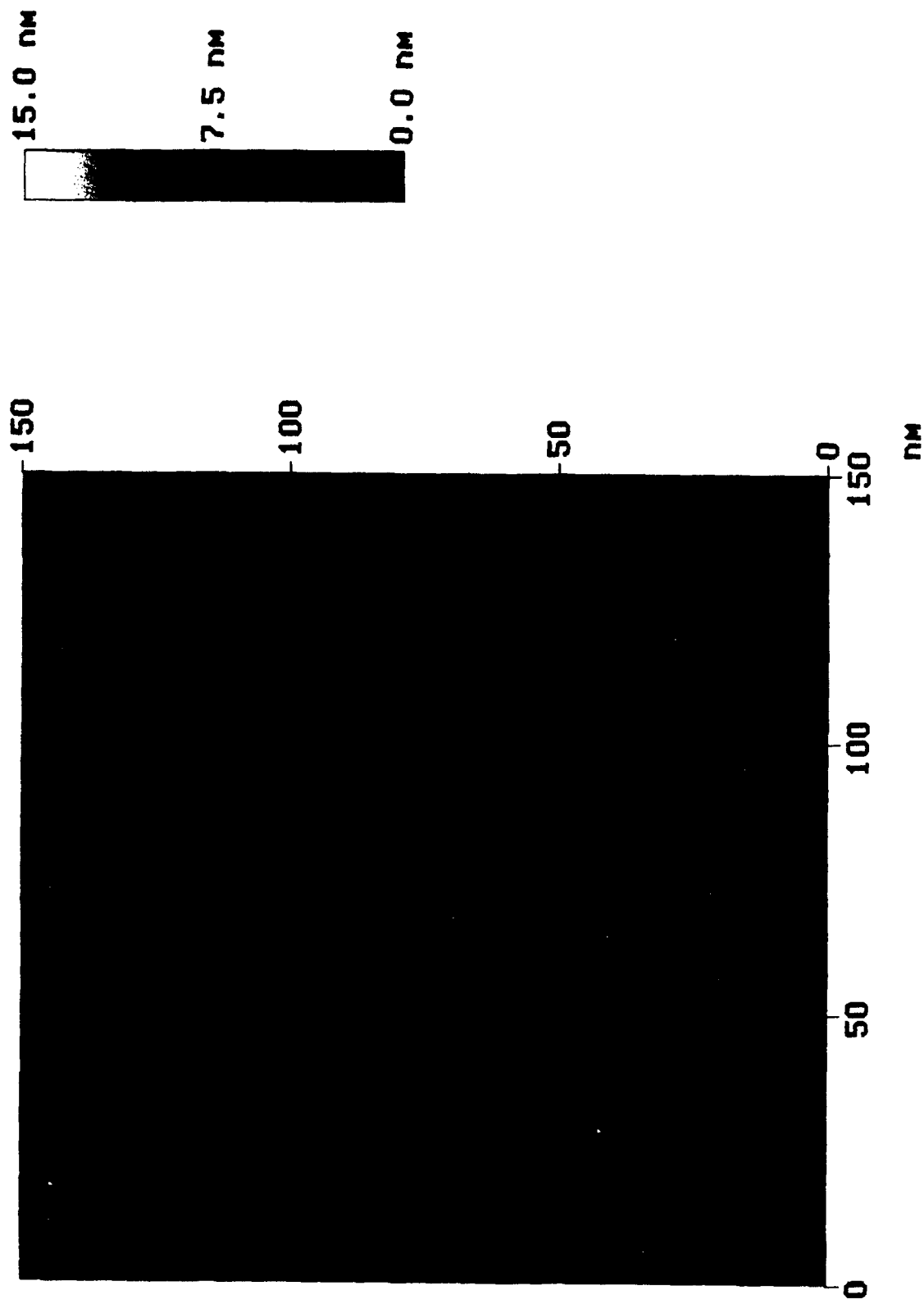


Figure 7a. AFM image at high magnification of two pits  
on an electrochemically corroded Al sample.

Vertical scale is 15.0 nm.

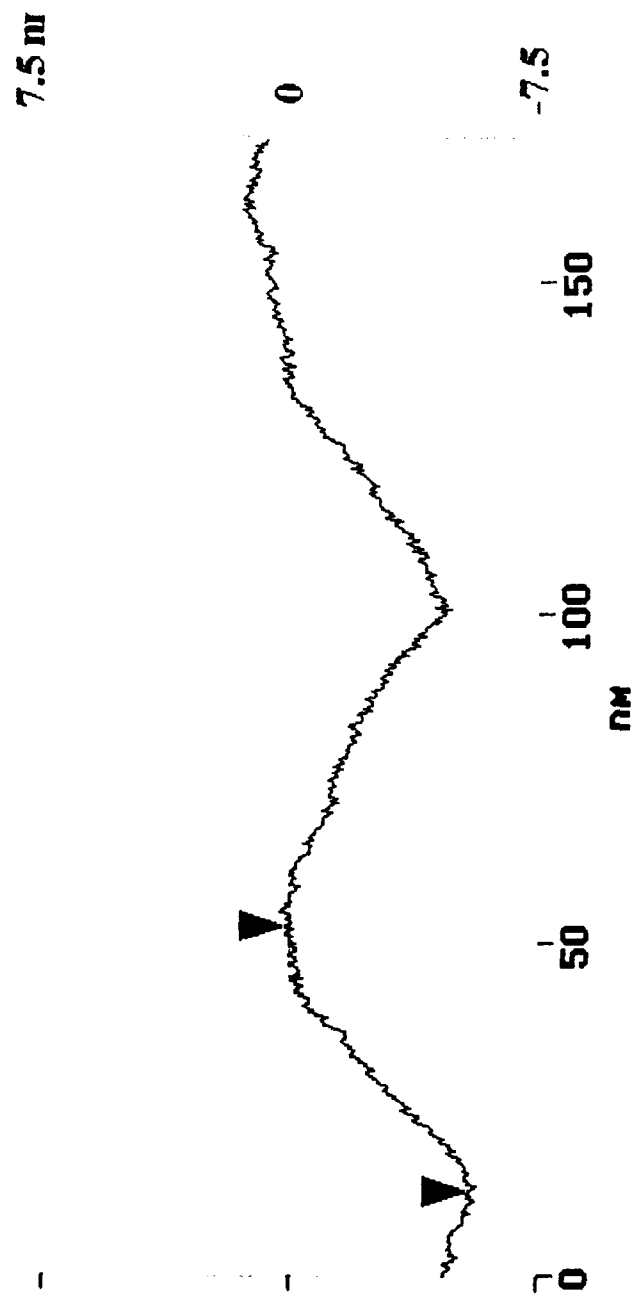


Figure 7b. Cross section of the two pits shown in Figure 7a.

was faster toward the bulk of the material (i.e., in the vertical direction) than along the surface (i.e., horizontal direction).

It is important to underline that these deep changes observed on the Al sample by AFM at the **nanometer scale** were introduced after holding the sample at the pitting potential for **only** 1 minute. Thus, the control of the electrode potential is fundamental in the determination of the mechanism of the accelerated corrosion process. On the other hand, AFM is shown to be sensitive to nanometer scale changes introduced at the initiation stage of the corrosion process.

#### **(iii) Identification of surface regions where corrosion is most likely to occur by the use of AFM**

Figure 5 shows an AFM image of a corroded Al sample with a high density of pits developed along two "lines" (cf., upper right corner). These "lines" correspond to two scratches already present before the pitting corrosion was electrochemically induced in the Al sample. Figure 5 indicates that the formation of pits induced electrochemically took place preferentially along surface features already present at the sample surface, such as scratches or steps.

#### **(iv) Impedance spectra of an aluminum sample before and during the pitting corrosion process in NaCl solution**

In order to describe the events which occur on a corroding surface before and during localized corrosion, the impedance spectroscopy technique was used. This technique was used to complement the information gained from the AFM experiments and to investigate the mechanism of the corrosion process.

The impedance spectra of an aluminum sample (mirror finish surface) were measured in 0.6 M NaCl solution. A small ac voltage was applied (20 mV rms) and the frequency of the signal was scanned between 10 KHz and 0.5 Hz. The spectra were recorded before, during, and after the pitting corrosion process took place on the Al sample. The pit formation was electrochemically induced by controlling the electrode potential. Figure 8 shows the Nyquist plot (imaginary ( $Z''$ ) vs real ( $Z'$ ) impedance components) obtained at the open circuit potential,  $V_{open}$  (i.e., before the electrochemically induced corrosion process) and at the potential before the pitting corrosion,  $V_{cor}^2$ . It was found that the features of the Nyquist plot could be taken as characteristic for the corrosion state of the Al sample: the corrosion process caused a significant decrease in the impedance values. These changes were even more pronounced

---

<sup>2</sup>  $V_{cor}$  was about 100 mV more cathodic than the pitting potential. At  $V_{cor}$ , a small anodic current (about  $30 \mu A cm^{-2}$ ) was observed, indicating that electrochemically induced corrosion was taking place.

when the spectra obtained at V open, where the corrosion process was not taking place were compared with the first spectrum taken at V<sub>cor</sub>, where the corrosion process was just initialized. The first two spectra taken at V<sub>cor</sub> (within 2 minutes) were also markedly different, indicating that the impedance data were very sensitive to the kinetics of the corrosion process. Impedance spectra taken successively during the corrosion process (after applying the pitting potential for 1, 2, 3, and 5 minutes) are also shown in Figure 8. At prolonged corrosion, the impedance spectra showed a decreased in both imaginary and real components.

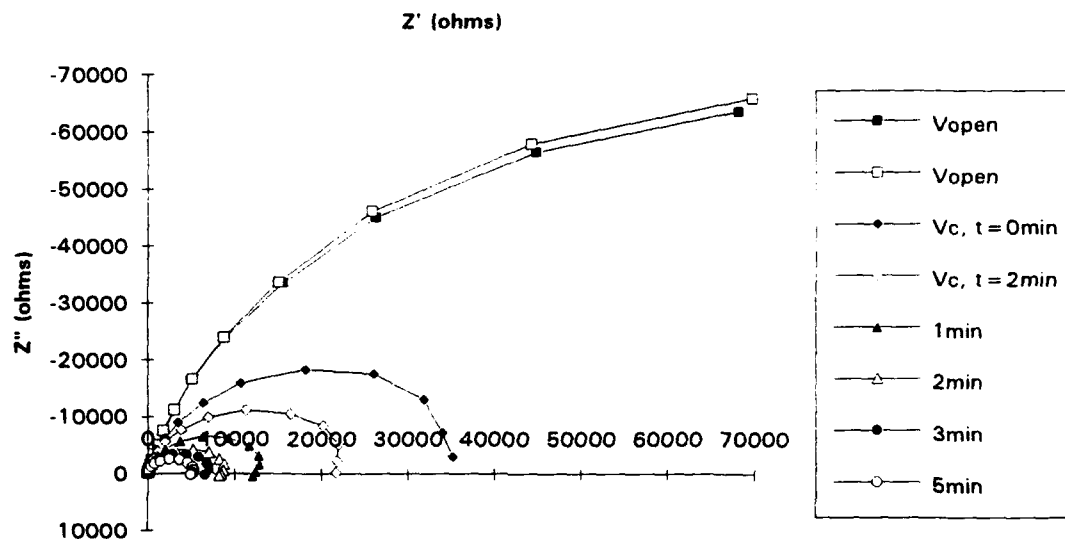


Figure 8. Nyquist plot obtained at different degrees of corrosion. For the last four plots, the electrode potential was held at the pitting potential (for 1, 2, 3, and 5 min., respectively). All the impedance spectra were obtained at V<sub>cor</sub>, except for the first two spectra, which were obtained at V<sub>open</sub>. The third and four plots were obtained at V<sub>cor</sub>, before the pitting potential was applied. Surface area was 0.283 cm<sup>2</sup>.

To answer the question if the observed corrosion effects on the impedance data were due only to changes in the surface area of the Al sample, the Bode plots were recorded. Figures 9 and 10 show the  $\log Z$  ( $Z = (Z'^2 + Z''^2)^{1/2}$ ) and angle ( $\text{angle} = \arctg(Z''/Z')$ ), respectively, as a function of the  $\log(\text{frequency})$ . Again, marked differences were obtained at different stages of the corrosion. These differences were obtained at frequencies below 100 Hz. In the angle vs  $\log(\text{frequency})$  plot a maximum was reached at about 100 Hz. At the open circuit potential (i.e., in the absence of corrosion) the angle vs  $\log(\text{frequency})$  plot was much broader than in the other cases. Similar observations were found by Mansfeld et al. (2), indicating that the impedance results can provide information on the degree of corrosion of an Al sample.

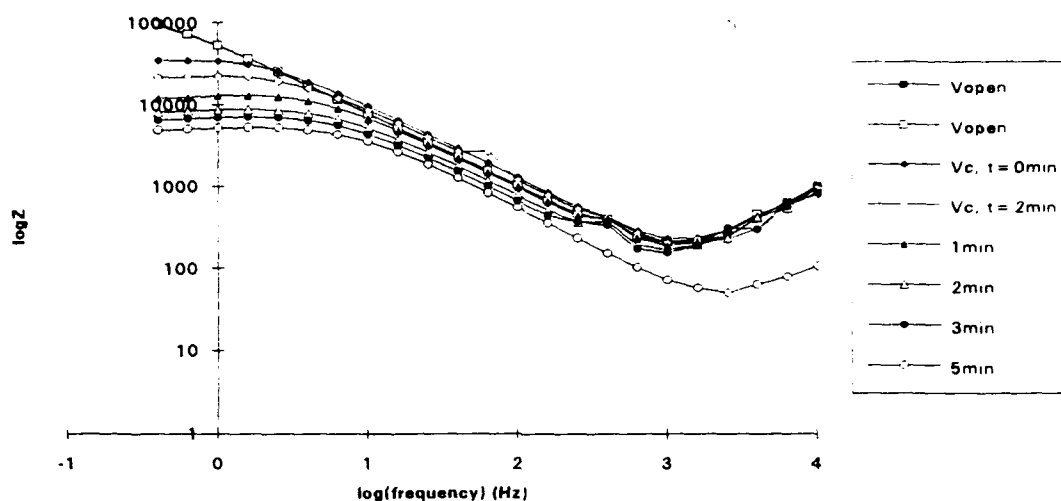


Figure 9. LogZ vs log(frequency) vs log(frequency) obtained at different degrees of corrosion. For the last four plots, the electrode potential was held at the pitting potential (for 1, 2, 3, and 5 min., respectively). All the impedance spectra were obtained at  $V_{cor}$ , except for the first two spectra, which were obtained at  $V_{open}$ . The third and four plots were obtained at  $V_{cor}$ , before the pitting potential was applied. Surface area was  $0.283 \text{ cm}^2$ .

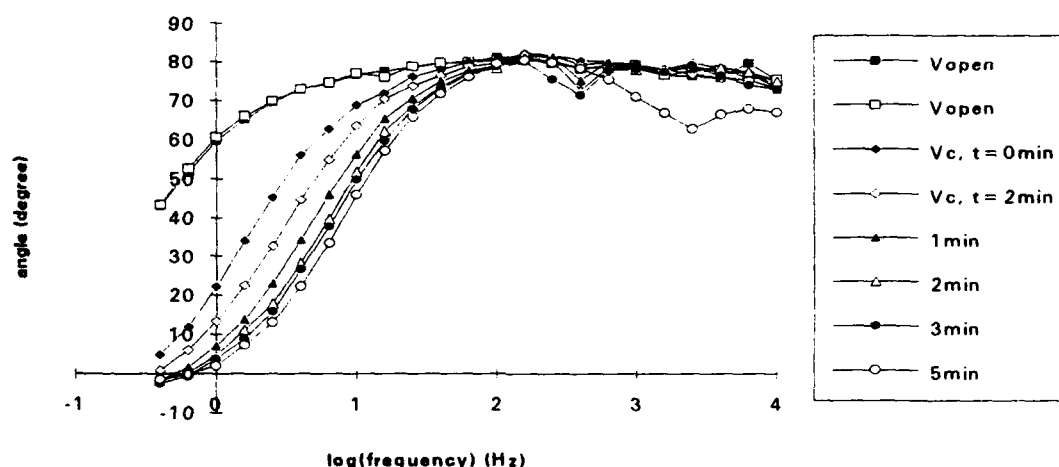


Figure 10. Angle vs log(frequency) obtained at different degrees of corrosion. For the last four plots, the electrode potential was held at the pitting potential (for 1, 2, 3, and 5 min., respectively). All the impedance spectra were obtained at  $V_{cor}$ , except for the first two spectra, which were obtained at  $V_{open}$ . The third and four plots were obtained at  $V_{cor}$ , before the pitting potential was applied. Surface area was  $0.283 \text{ cm}^2$ .



It is interesting to compare the results obtained by AFM and the impedance spectroscopy technique. After 1 minute of accelerated electrochemical corrosion (i.e., at the pitting potential) both the AFM images and the impedance data showed characteristic changes, and for the pitting initiation process. The AFM images provided information on the nanometer scale whereas the changes in the impedance data provided a way of monitoring the corrosion process by macroscopic parameters.

**(v) Identification of a critical frequency where the change in the impedance parameters caused by the corrosion of the aluminum sample exhibited a maximum**

Figures 9 and 10 shows the Bode plots as a function of the log(frequency). In both cases, it is observed that marked differences between different degree of corrosion were obtained at frequencies below 100 Hz. This result indicates that in order to detect the degree of the corrosion, the impedance analysis could be reduced to only a few characteristic frequencies, thus reducing the time for data acquisition.

#### **WORK TO BE PERFORMED DURING NEXT REPORT PERIOD**

Real time, *in situ* AFM imaging of the corrosion of Al sample at the open circuit potential and under accelerated electrochemical corrosion is planned. Same experiments will be carried out for Al alloy samples (Al 7075). Impedance spectroscopy analysis, similar to the one presented in this report, will be carried out for the alloy samples.

#### **REFERENCES**

1. M. Szklarczyk and J.O'M. Bockris, J. Electrochem. Soc., **137** (1990) 452.
2. F. Mansfeld, S. Lin, S. Kim and H. Shih, J. Electrochem. Soc., **137** (1990) 78.